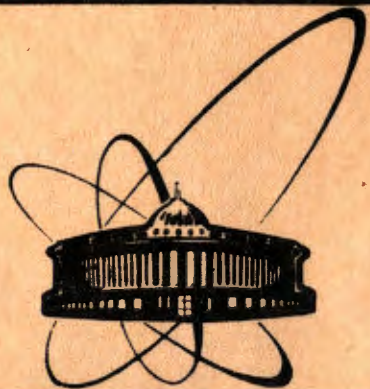


92-250



сообщения
объединенного
института
ядерных
исследований
дубна

E1-92-250

A.D.Kovalenko, Yu.A.Panebratsev, S.S.Shimanskiy,
V.I.Yurevich, R.M. Yakovlev*

EXPERIMENTAL SETUPS AND METHODS
TO OBTAIN NEW NUCLEAR DATA AT INTERMEDIATE
AND HIGH ENERGIES

*V.G.Khlopov Radium Institute, St.Petersburg, Russia

1992

INTRODUCTION

During many years fundamental problems of nuclear and hadron physics have been investigated at the Laboratory of High Energies of the Joint Institute for Nuclear Research (LHE/JINR). With this aim some modern physical methods and setups have been developed and designed on the basis of the main accelerator of the LHE - the synchrophasotron. On the one hand, the existence, of intense beams of relativistic protons and light-mass heavy ions with $A \leq 28$ over a broad energy range of $(0.3-3.6)A$ GeV and, on the other hand, a lot of experimental setups gives the LHE the status of one of the leading scientific centers in the field of relativistic nuclear physics. The possibilities for research will be substantially expanded after putting the new superconducting synchrotron, Nuclotron, into operation. The characteristics of the beams of the LHE accelerator complex are shown in table 1 [1].

Table 1. Relativistic nuclear beams at the LHE accelerator complex

Beam*	Intensity (particles per cycle)	
	Synchrophasotron ($P_{\max} = 4.5$ GeV/c/N)	Nuclotron ($P_{\max} = 7$ GeV/c/N)
p**	$4 \cdot 10^{12}$	$2 \cdot 10^{11}$
d**	$1 \cdot 10^{12}$	$1 \cdot 10^{11}$
^4He	$5 \cdot 10^{10}$	$1 \cdot 10^{10}$
^7Li	$2 \cdot 10^9$	$3 \cdot 10^9$
^{12}C	$1 \cdot 10^9$	$1 \cdot 10^{11}$
^{24}Mg	$2 \cdot 10^7$	$6 \cdot 10^9$
^{40}Ar	-	$3 \cdot 10^7$
^{84}Kr	-	$2 \cdot 10^7$
^{131}Xe	-	$1 \cdot 10^7$
^{238}U	-	$\sim 10^6$

* Some available ion beams are only presented.

** At present the operation intensities of p-, d-beams are limited at a level of 10^{11} p/cycle by dosimetry service.

Recently the expert groups have formulated the requirements to nuclear data in the intermediate energy region [2,3]. At present the set of nuclear data over this energy range is very poor and far from fullness. So, many efforts are undertaken at different laboratories to create the base of intermediate-energy nuclear data needed for a lot of important applications in science and technology. However, the LHE accelerator complex has unique possibilities for such investigations nowadays.

In this paper an attempt is made to pay attention to the possibility of using the LHE potentials to obtain different nuclear data at intermediate and high energies.

HADRON AND HARD PHOTON SPECTROMETERS

New possibilities for an experimental search and study of new forms of nuclear matter are connected with the appearance of high-energy heavy-ion accelerators. The extreme high-dense and high-temperature nuclear matter states have a very short lifetime and in an evolution process they disintegrate by hadron and hard photon emission with specific characteristics. With some probability these states are produced in nucleus-nucleus collisions in a small volume within the overlapped region.

The described experimental setup has been made for a systematic study of the possibility and conditions of strengthening the display of the effects of new nuclear matter form and their investigation [4]. In future we are planning to measure the correlation of $\gamma/\pi/n/p/d/t$ production differential cross sections in a wide region of the energy and mass of colliding nuclei at different angles. Our special interest is to research hard photon and pion production at ion energies of 100 ± 500 MeV/A including the subthreshold effects and to study low-energy neutron and gamma emission in central nucleus-nucleus collisions.

This setup placed on external ion beam channel N38 of the Synchrophasotron consists of a tandem of the $\Delta E-E$ and $t-E$ spectrometers. These spectrometers arranged one after another along the beam direction can operate as independent setups with their targets T1 and T2 as shown in fig.1.

The ion beam is determined and monitored by a system of beam counters, and its profile and position are monitored by a multiwire proportional chamber, MWPC. Beam signals are generated as a coincidence of the beam counters:

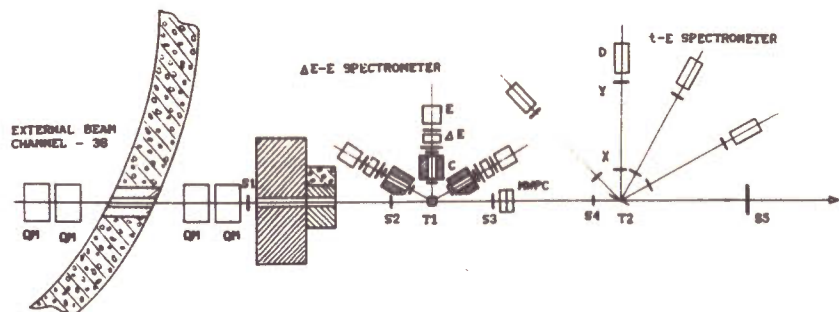


Fig.1. Schematic view of the hadron and hard photon spectrometer tandem.

"BEAM" = $\begin{cases} S1*S2 & \text{- for the } \Delta E\text{-E spectrometer} \\ S1*S3*S4 & \text{- for the t-E spectrometer.} \end{cases}$

Central nucleus-nucleus collisions are separated in a pulse height analysis using counters S3 and S5 for the $\Delta E\text{-E}$ and t-E spectrometers, respectively. Nuclear fragments going to forward angle region from 0° to 5° are detected by these counters. The pulse height spectrum (detector S5 with a 5 mm plastic scintillator) for 1-GeV $A^{12}\text{C}$ -ion fragmentation on a 15 mm lead target is shown in fig.2. The peaks in the plot correspond to the registration of projectile fragments with different charge.

$\Delta E\text{-E}$ SPECTROMETER

The main aim of this setup is to measure the double differential cross section of hard photon production in nucleus-nucleus collisions. But we are also planning to detect charged hadrons by the $\Delta E\text{-E}$ technique. This spectrometer has three identical detec-

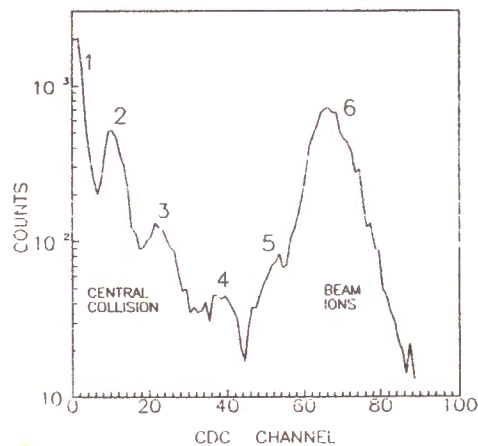


Fig.2. Pulse-height distribution of fragments in the forward direction measured with counter S5 for 1-GeV $A^{12}\text{C}$ -ion fragmentation on the lead target.

tor systems, and each of them is a gamma-telescope based on large volume NaJ(Tl) detectors. The detector system of the gamma-telescope is given in table 2. The first NaJ(Tl) detector 1.56 X_0 thick is a high-energy gamma-ray active converter. The electron-photon cascade passing through a thin plastic counter (Z) is absorbed in a large NaJ(Tl) detector (E). So, the gamma-event is $\bar{V} \cdot \Delta E \cdot Z \cdot E$ coincidence producing a signal "G". A charged particle signal "Z" is given by $X \cdot Y \cdot \Delta E$ coincidence. The ΔE detector is placed at a 50 cm distance from target T1.

Table 2. Gamma-telescope detector system

Detector	Scintillator	Signal
X	10x10x3 mm plastic	timing
Y	8x8x5 mm plastic	timing, pulse-height
V	150x150x5 mm plastic	timing (veto-counter)
ΔE	140x140x40 mm NaJ(Tl)	timing, pulse-height
Z	130x130x5 mm plastic	timing
E	$\phi 150 \times 150$ mm NaJ(Tl)	timing, pulse-height

The lead collimator (its thickness is 20 cm; and the aperture, $\phi 6$ cm) is between two thin counters (X and Y), and photons fall only on a central part of the ΔE detector-converter. This gamma-telescope overlapping the energy region from 30 to 300 MeV has been calibrated using cosmic muons. Hard photon detection has been studied by the gamma-telescope using the GEANT 3 code [5]. The telescope response to 90-, 180- and 300-MeV photons is given in fig.3. The energy dependence of the gamma-telescope efficiency is given in fig.4. A strong background discrimination is realized 1) with a fast coincidence of pulses of the ΔE , Z and E detectors within 20 ns; 2) using a short time interval of about 1 ns on a time-of-flight scale and 3) using the veto-counter for charged particle discrimination. The use of a thin Cherenkov counter instead of a plastic counter (Z) can give a stronger discrimination of high-energy neutrons. In table 3 our gamma-telescope is compared with other high-energy gamma-spectrometers [6-10].

t-E SPECTROMETER

This multidetector spectrometer is used for time-of-flight measurements of double differential cross sections of hadron production with off-line separation of π^\pm , p, d and t by t-E

Table 3. A comparison of the hard photon spectrometers

Year [Reference]	γ -detector	E_{γ} (MeV)	ϵ_{γ} (%)	FWHM (%)	FWHM(TOF) (ns)
1990	present detector	30-300	15-43	20	0.7
1987 [6]	veto-counter BaF ₂ (ϕ 10x14 cm)	8-85	15-30		0.7
1988 [7]	veto-counter, BaF ₂ (6x4x1 cm), two NE102 (2mm) NaJ(Tl) (ϕ 15x20 cm)	>20			
1988 [8]	veto-counter, five Pb-glass detectors	20-150	9-20	25-35	2.5
1988 [9]	veto-counter, BaF ₂ (60 cm ³), BGO (750 cm ³)			14	0.5
1989 [10]	veto-counter, Cu/SCG1-C glass (0.5 Xo conver- ter), two MWPC, plastic, SCG1-C glass (15x15x42.5 cm)	20-300	20		

(time-of-flight - pulse height) analysis. Charged particles are measured by the telescope (X, Y, D) consisting of two thin plastic counters and a thick plastic detector (E). Neutron emission is studied with the aid of large plastic scintillators (D), and the counters (Y) are used as veto-counters for charged particle discrimination. A brief description of the single detector system is given in table 4. The t-E plot for the interaction of 1-GeV A ⁶Li-ions with a carbon target is shown in fig.5. The efficiency of the neutron detector for two threshold values of 10 and 30 MeV is shown in fig.6. Overlapping energy region for hadrons is: 20-120 MeV for pions;

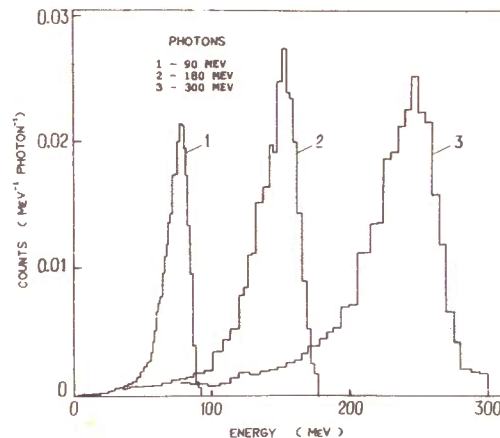


Fig.3. Response distributions of the gamma-telescope for 90, 180, 300 MeV photons.

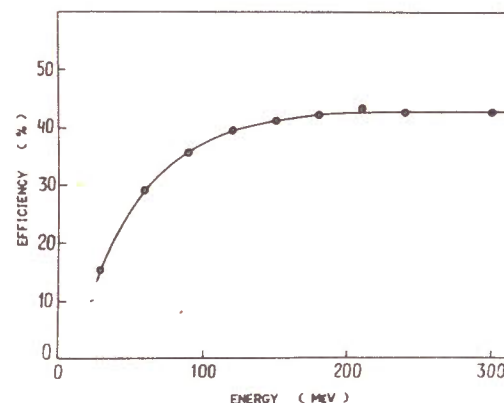


Fig.4. Energy dependence of the gamma-telescope efficiency.

Table 4. Detector system of t-E spectrometer

Detector	Scintillator	Signal
X	100x100x3 mm plastic	timing
Y	130x130x5 mm plastic	timing
D	ϕ 120x200 mm plastic	timing, pulse-height

50-300 MeV for hydrogen ions and 20-500 MeV for neutrons. For both spectrometers data accumulation is performed on-line with a computer.

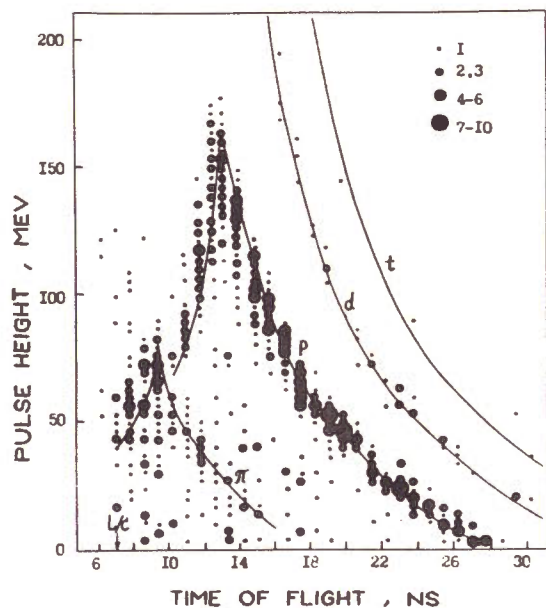


Fig. 5. The t-E plot measured at 30° with 1 GeV $A^6\text{Li}$ -ions and carbon target. Points - the experiment, curves - the calculation.

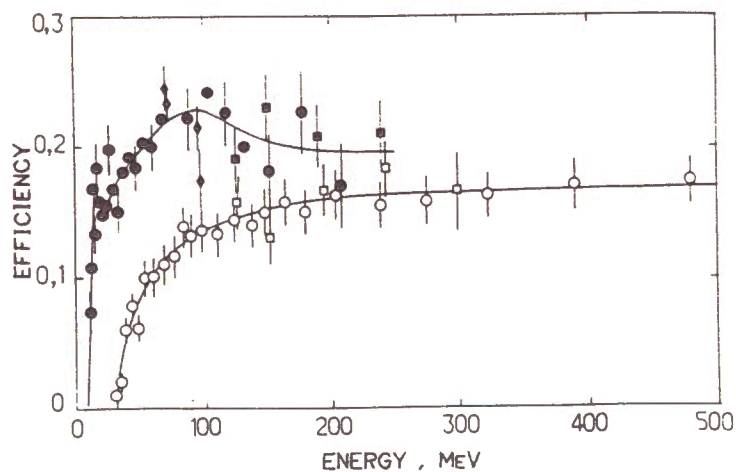


Fig. 6. Efficiency of the neutron detector for two threshold values of 10 and 30 MeV.

MAGNETIC SPECTROMETER

The two-arm magnetic spectrometer, DISC, was designed for inclusive and correlation measurements of the cross sections of different charged particle production in proton-nucleus and nucleus-nucleus interactions. The main research direction of this physical setup is to study the process of cumulative hadron production on different nuclei and to investigate the lightest-mass nuclei structure at small distances. Two magnetic arms of the DISC are intended for the registration of target fragmentation products in an inclusive experiment. The coincidence of these two spectrometers allows one to carry out correlation measurements. This experimental setup and its parameters were described in detail in ref. [11,12]. So, the basic characteristics of the spectrometer are only given here. A scheme of the setup is shown in fig. 7.

The first arm of the setup is a rotating magnetic spectrometer, (M1), used to register target fragments (π^\pm , K^\pm , p, p, d, t, ^3He and ^4He) at angles from 60° to 180° relative to the beam direction and in a momentum region from 150 MeV/c to 1800 MeV/c. The momentum resolution is $\pm 4\%$ and the entrance solid angle $2 \cdot 10^{-4}$ sr. Useful events are separated in independent measurements of the time of flight on two flight paths of 3.8 m and 1 m (the standard error is 260 ps). The ionization losses in the scintillators and light output in the Cherenkov counters with solid-state radiators are measured to rise the separation possibility of the spectrometer. Charged pions with a momentum of above 900 MeV/c are detected with a gas-filled threshold Cherenkov counter. Spectrometer M1 allows the identification of secondary particles to be carried out at a large beam intensity (to $\sim 5 \cdot 10^{11} \text{ s}^{-1}$) using a target with a thickness of $\leq 10 \text{ g/cm}^2$.

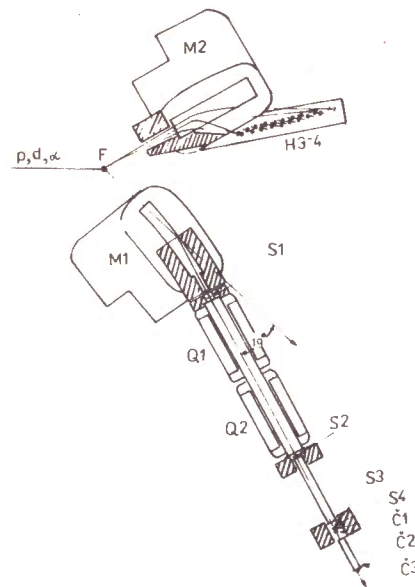


Fig. 7. Scheme of the two-arm magnetic spectrometer DISC.

Rotating magnetic spectrometer, M2, allows one to detect pions, protons and deuterons in a momentum region of 50 ± 800 MeV/c ($\Delta p/p = 1.2$) and 1000 ± 1500 MeV/c ($\Delta p/p = 0.2$) overlapping the interval of angles from 20° to 140° relative to the beam direction. Useful events are separated as in spectrometer M1 using the time of flight technique and the ionization loss. Spectrometer M2 operates in coincidence with magnetic spectrometer M1. This regime makes it possible to successfully separate πp -, pp - and dp -coincidences at a beam intensity of $\sim 10^{10} \text{ s}^{-1}$ and a target thickness of 1 g/cm^2 . A combination of these two spectrometers (M1 and M2) is also used to study two-particle correlations in cumulative particle production and to measure the correlation function for πp -coincidence in the effective-mass region corresponding to the appearance of cumulative Δ -isobars.

Further on we plan to use in correlation measurements the magnetic spectrometer DISC in common with the nonmagnetic hadron spectrometer described above. It should be particularly noted that the setup DISC has as its element a cryogenic target which can be filled with liquid hydrogen, deuterium or helium. The presence of such a target allows one to carry out both investigations with lightest-mass nuclei and to obtain (using $^1, ^2\text{H}$ targets and proton and deuteron beams) information about

the "elementary" nucleon-nucleon interaction. This is very important for theoretical calculations and taking into account collective effects connected with the specificity of nucleus-nucleus interactions.

NEUTRON SPECTROMETER

At present the time-of-flight neutron spectrometer consists of three identical detector systems at three different angles and

a detector for measurements in a low-energy region. Measurements can be carried out with stylben detectors or large plastic scintillators. A schematic drawing of the target-detector arrangement on the external beam channel of the Synchrophasotron is given in fig.8. Neutron emission is studied at angles of $30, 90$ and 150° using three types of neutron detectors which cover a very broad energy region from about 0.2 MeV to a beam energy containing more than 95% of all emitted neutrons. So, we can study all stages of neutron emission: cascade, pre-equilibrium and equilibrium. The thin plastic scintillators as veto-counters for charged particles are placed in front of all the detectors. A short characteristic of the neutron spectrometer detector system is given in table 5.

The n - γ pulse-shape discrimination is employed for the stylben detectors. Neutron- and gamma-events are separated at the stage of off-line data analysis. As an example, two time-of-flight spectra (without and with n - γ separation) measured using a fast ionization chamber with a layer of ^{252}Cf as the source of neutrons and gamma-quanta are shown in fig.9. Many efforts have been undertaken to determine accurately the efficiency of the neutron detectors [13]. Figure 10 presents the efficiency data for the D1, D2 and D3 detectors with threshold values of $0.1, 1$ and 30 MeV , respectively. The typical time resolution is about 0.5 and 1 ns/m (FWHM of a prompt γ -ray peak)

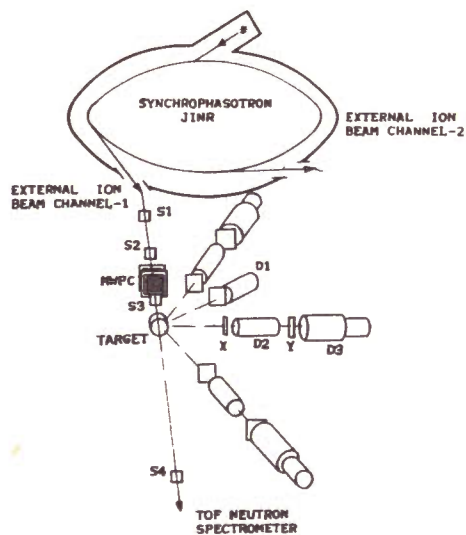


Fig.8. Schematic drawing of target-detector arrangement for the TOF neutron spectrometer.

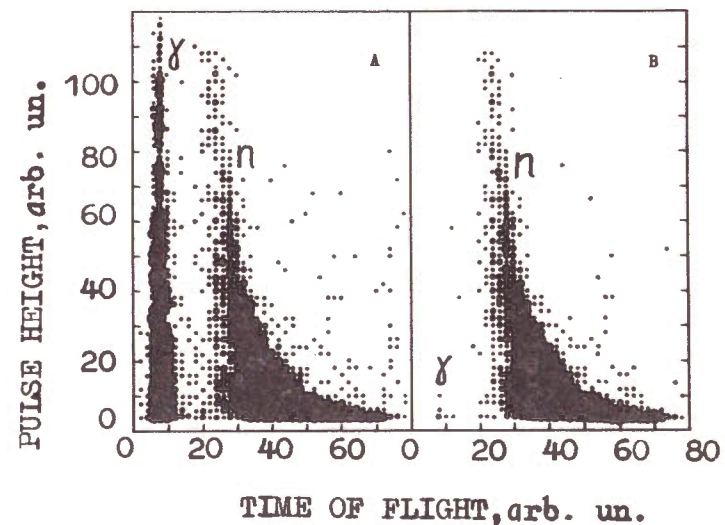


Fig.9. Two time-of-flight spectra measured by the fast ionization chamber with ^{252}Cf layer: (A) - without and (B) - with n - γ discrimination.

Table 5. Detector system of Neutron Spectrometer

Detector	Scintillator	Energy region	Signal
COUNTERS			
X	100x100x3 mm plastic	-	timing
Y	130x130x5 mm plastic	-	timing
DETECTORS			
D1	φ40x10 mm stylben	0.2-3 MeV	timing, pulse-height 1 pulse-height 2
D2	φ50x50 mm stylben	2-30 MeV	timing, pulse-height 1 pulse-height 2
D3	φ120x200 mm plastic	20-500 MeV	timing, pulse-height

for the plastic and stylben detectors, respectively. The position and profile of the beam in front of the target are monitored by means of a multiwire proportional chamber, MWPC. The

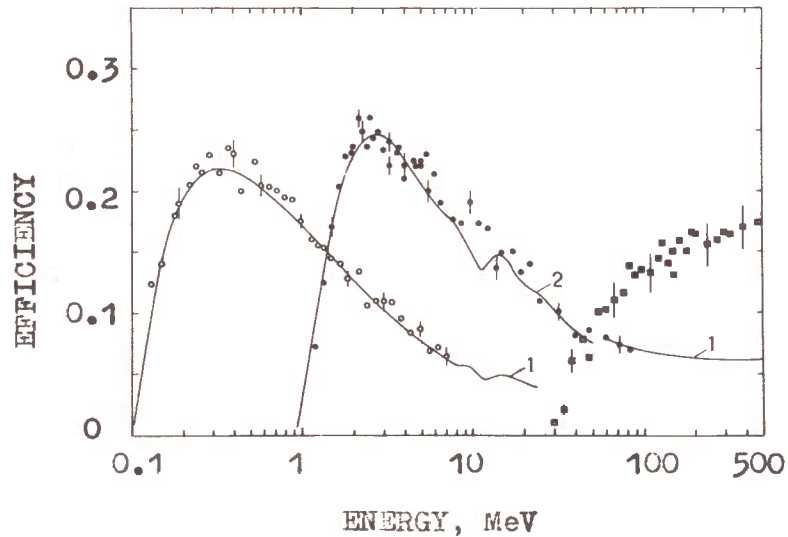


Fig.10. Efficiency of neutron detectors D1, D2 and D3 with threshold values of 0.1, 1 and 30 MeV, respectively. The points - experimental data, the curves - results of calculations.

beam size is typically 20 mm (FWHM) in the vertical and horizontal directions. The experimental method and setup were described in detail in ref. [14]. The present setup is compared with some other TOF neutron spectrometers [15-18] in table 6.

As an example of experimental results, the neutron spectra at 90° from thick lead targets 8x8x8 cm³ and φ20x20 cm³ in size bombarded by 2- and 2.55-GeV protons, respectively, and different 1-GeV A ions are shown in fig.11. The histogram is the calculation for the proton beam by the code SITHA [19,20].

Table 6. Comparison of the TOF Neutron Spectrometers

Laboratory [Ref.]	Year	Beam	Energy region (MeV)	Number of arms	Neutron detector	n/γ*	Z**
LANL [15]	1980	p(0.8 GeV)	0.9-500	1	NE-213	Y	N
LNPI [16]	1981	p(1 GeV)	>10	1	plastic	N	N
ITEP [17]	1980	p(1-10 GeV)	10-300	8	plastic	N	Y
KFK [18]	1987	p(0.59 GeV)	0.9-500	3	NE-213	Y	N
JINR [14] (RI)	1990	p(1-10 GeV) d-Ar (0.5-3.6 GeV A)	0.2-1000	3	stylben, plastic	Y N	N Y

* The possibility of n/γ discrimination.

** The possibility of charged particle separation.

THRESHOLD DETECTOR TECHNIQUE

About six years ago we started to develop the threshold detector technique extending it to a high energy region. At present there is no other experimental method with such possibilities for a fast analysis of spatial-energy neutron (hadron) distributions under different experimental and geometric conditions. Several tens or hundreds of detectors can be used for neutron/hadron field investigations simultaneously. An automatic count of tracks allows one to perform express data processing (single threshold detector processing takes only 4 minutes). This method is described in detail in [21,22,23]. The neutron/hadron detector is a set of threshold detectors and consists of well-known fission detectors with about 1 mg/cm² layers of ²³⁵U, ²³⁷Np, ²³⁸U, ²³²Th, ²⁰⁹Bi and new high threshold spallation detectors with thick layers of Ti, Cu and Cd.

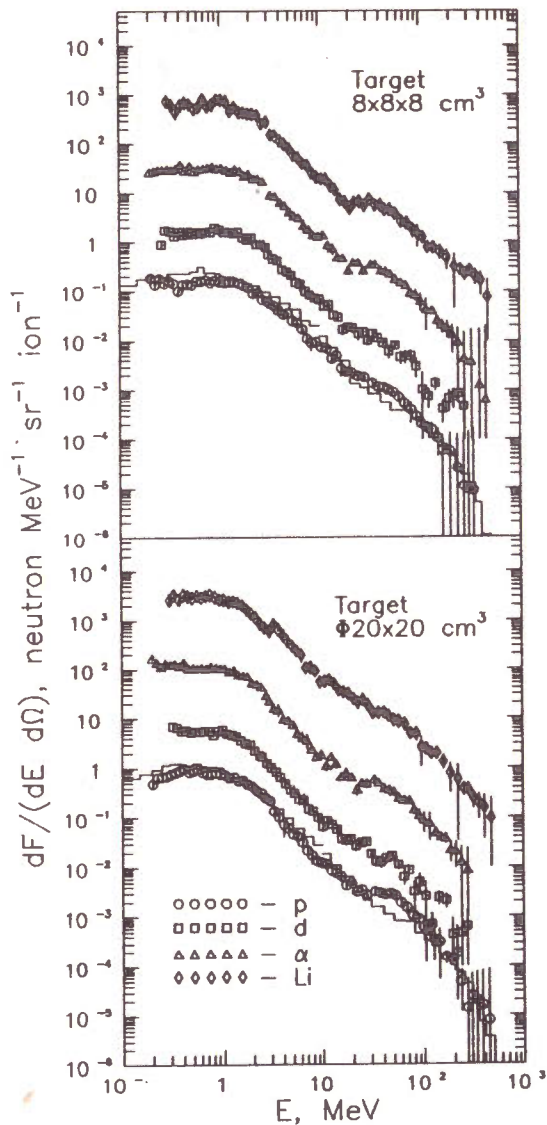


Fig.11. Neutron spectra at 90° for two thick lead targets bombarded by 2 GeV and 2.55 GeV protons and different 1 GeV A ions. The values for d, α and ${}^6\text{Li}$ -ions are increased by factors of 10, 100 and 1000, respectively.

Fission and spallation fragments produced by neutrons/hadrons are registered by means of solid state nuclear track detectors (SSNTD) based on 6- μm polyethyleneterephthalate (PETP). The efficiency for fission detectors was calculated using the known values of fission cross sections. But for spallation detector it was measured using a proton beam assuming the independence of efficiency of the kind of nucleon. The efficiency of the full set of threshold detectors is shown in fig.12. Total information about this method is shown in table 7.

The test measurements were made in a neutron field of the spallation neutron source (the extended lead target $\phi 20 \times 20$ cm bombarded by a proton beams of the Synchrophasotron). The measurements have shown a good agreement with the time-of-flight results. The neutron distributions are calculated from the experimental results by the iteration code RESTOR [21]. As an example, the angular distribution of neutrons with different energies produced by

Table 7. Characteristics of the threshold detectors method

Overlaped energy region	thermal - several GeV
Typical number of the hadron detectors in single experiment	tens - hundreds
<u>SSNTD (PETP) characteristics</u>	
Sensitivity to particles:	
3-MeV neutrons	$< 10^{-12}$
14-MeV neutrons	$< 10^{-11}$
5.47-MeV α -particles (2 π -geometry)	$< 5 \cdot 10^{-11}$
fission fragments (2 π -geometry)	0.515
Effective nuclear charge threshold (Z_{th})	5
<u>Detector characteristics</u>	
Maximum value of efficiency:	
of 1 mg/cm fission detector	$\sim 3 \cdot 10^{-6}$
of spallation detector	$\sim 4 \cdot 10^{-7}$
Dimension:	
of the threshold detector	$\phi 19 \times 0.3$ mm
of hadron detector	$\phi 20 \times 3$ mm
<u>Detector processing</u>	
Counting time for one SSNTD	3 min.
Total time of data processing for 100 hadron detectors (~ 600 threshold detectors):	
using one automated counter	30 days
using five automated counters	7 days
Optimal statistic	2000-4000 cm
Typical total methodical error of hadron fluence:	
low-energy region	6-10%
high-energy region	15-25%
Possibility of reprocessing of SSNTD	yes
Time of information storage in SSNTD	years

3.65-GeV protons in the large lead target $\phi 20 \times 60$ cm is shown in fig.13.

This technique has been used to research the spallation neutron source in the measurements with $1 \div 3.7$ -GeV protons

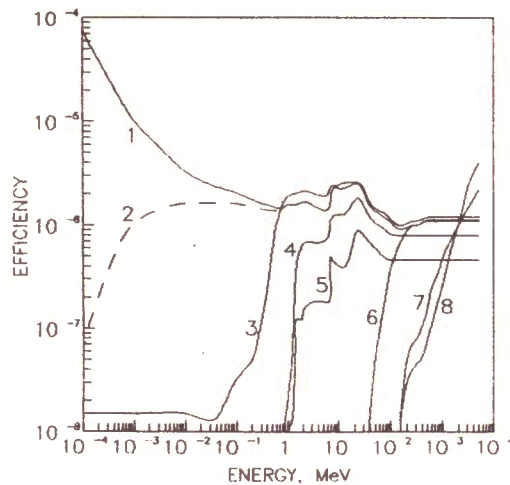


Fig.12. Efficiency of the full set of threshold detectors consisting of fission detectors with 1 mg/cm^2 fissile layers of ^{235}U (1), ^{235}U with a 2 g/cm^2 boron filter (2), ^{237}Np (3), ^{238}U (4), ^{232}Th (5), ^{209}Bi (6) and spallation detectors with thick layers of copper (7) and cadmium (8). The values of curves (6-8) are increased by a factor of 10.

and deuterons, and recently the results have been reported [24]. We are planning to develop this method in the future and should like to extend its applications in science and technology. As we can see, possible applications can be connected with the study of doses and hadron fields on accelerators, damage of materials, spallation neutron sources, hadron calorimeter design and so on.

CONCLUSION

A comparison of the described spectrometers with others available at different laboratories shows that these setups are strong instruments for physical research and their combination has exceptional possibilities both for a comprehensive study of secondary particle production in thin and thick targets by high-energy ions and for precise measurements of neutron, charged hadron and hard photon spectra and spatial-energy distributions of the flux density of neutrons/hadrons. In other words, these spectrometers can be considered as a basic experimental facility for high energy nuclear data measurements over a broad energy region for incident heavy ions and for secondary particles. Taking into account the exceptional beams of the JINR accelerators and a great demand on such results, in particular for incident energies above several hundred MeV per

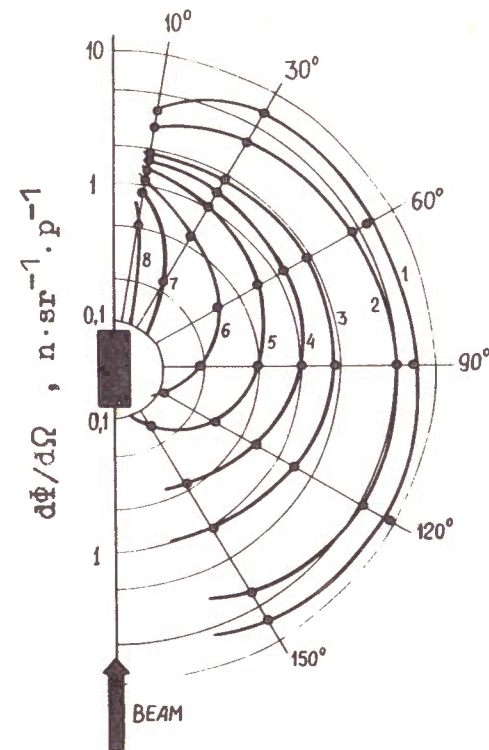


Fig.13. Neutron angular distributions for different energy groups measured with a large lead target and 3.65 GeV protons. Curves 1÷8 correspond to the flux density of neutrons with an energy above 0, 1, 6, 20, 50, 100, 250 and 500 MeV, respectively.

nucleon, the authors believe that the developed experimental methods and setups will make their significant contribution to international efforts on the formation of a bank of high-energy nuclear data.

REFERENCES

1. Issinsky I.B., Mikhailov V.A. - JINR P1-92-2, Dubna, 1992.
2. Matsurobu H. - Proc.1989 Seminar on Nuclear Data, Feb.1990, JAERI-M, 90-025, 1990, p.167.
3. Ed. Kocherov N.P. - Intermediate Energy Nuclear Data for Applications, INDC (NDS)-245, IAEA, Vienna, 1991.
4. Yurevich V.I. et al. - JINR E1-92-249, Dubna, 1992.
5. Brun R. et al. - GEANT 3 DATA Handling Division, CERN DD/EE/84-1, 1987.

6. Hingmann R. et al. - Phys. Rev. Lett., 1987, v.58, p.759.
7. Kwato Njock M. et al. - Phys. Lett., 1988, v.B207, p.269.
8. Tam C.L. et al. - Phys. Rev. C, 1988, v.38, p.2526.
9. Arctaedins Th. et al. - 3d Int. Conf. on Nucleus-Nucleus Collisions, 1988 Saint-Malo, 1988, p.94.
10. Chiavassa E. et al. - Nuovo Cimento, 1989, v.101A, p.805.
11. Avericheva T.V. et al. - JINR 1-11317, Dubna, 1978.
12. Averichev G.S. et al. - JINR Rapid Communications, 1[37]-89, Dubna, 1989.
13. Lyapin V.G. et al. - Preprint R1-217, M.: Atominform, 1990.
14. Kirilov A.D. et al. - JINR P13-90-193, Dubna, 1990.
15. Howe S.D. et al. - Proc. Int. Conf. on Nuclear Cross Sections for Technology, Knoxville 1979, NBS sp.pub.594, 1980, p.413.
16. Baturin V.N. et al. - VANT: Nuclear Data. M.: Atominform, 1981, v.2, p.6.
17. Bayukov Yu.D. et al. - Preprint ITEP-159, ITEP-16, M., 1980.
18. Cierjacks S. et al. - Phys. Rev. C., 1987, v.36, p.1976.
19. Daniel A.V. - Preprint R1-181, M.: Atominform, 1984.
20. Daniel A.V. et al. - JINR E1-92-174, Dubna, 1992.
21. Vorobyev I.B. et al. - Preprint R1-218, M.: Atominform, 1990.
22. Vorobyev I.B. et al. - JINR P13-90-194, Dubna, 1990.
23. Yurevich V.I. et al. - JINR E1-92-189, Dubna, 1992.
24. Nikolaev V.a. et al. - ICANS-XI, Proc. Int. Collaboration on Advanced Neutron Sources, Tsukuba 1990, KEK, 90-25, 1991, v.1, p.612.

Received by Publishing Department
on June 15, 1992.

Коваленко А.Д. и др.

E1-92-250

Экспериментальные установки и методики
для получения новых ядерных данных
при промежуточных и высоких энергиях

Дается краткое описание новых экспериментальных установок для всестороннего изучения процесса образования вторичных адронов, нейтронов и жестких фотонов в протон- и ядро-ядерных столкновениях, а также для получения ядерных данных при промежуточных и высоких энергиях на пучках синхрофазотрона ЛВЭ ОИЯИ. Необходимые для различных приложений ядерные данные могут быть получены на имеющихся пучках в диапазоне энергий налетающих ядер с $A \leq 28$ (0,3-3,6) А ГэВ. Возможности установок будут значительно расширены после ввода в действие нового сверхпроводящего синхротрона - нуклотрона. Описанные установки и экспериментальные методики разработаны сотрудниками Лаборатории высоких энергий и Радиового института им. В.Г. Хлопина.

Работа выполнена в Лаборатории высоких энергий ОИЯИ.

Сообщение Объединенного института ядерных исследований. Дубна 1992

Kovalenko A.D. et al.

E1-92-250

Experimental Setups and Methods
to Obtain New Nuclear Data at Intermediate
and High Energies

A short description of new experimental setups designed for a comprehensive study of the production process of secondary hadrons, neutrons and hard photons in proton- and nucleus-nucleus collisions and also for obtaining nuclear data at intermediate and high energy beams of the Dubna synchrotron is given. Nuclear data needed for different applications can be obtained at available beams with (0.3-3.6) A GeV energy of incident nucleus with $A \leq 28$. The possibilities of setups will be substantially expanded after putting the new superconducting synchrotron, the Nuclotron, into operation. These setups and experimental methods have been developed by collaborators of the Laboratory of High Energies (JINR) and V.G. Khlopin Radium Institute.

The investigation has been performed at the Laboratory of High Energies, JINR.

Communication of the Joint Institute for Nuclear Research. Dubna 1992